Gravitating σ model solitons

Yoonbai Kim*
Department of Physics and Institute of Basic Science, Sungkyunkwan University, Suwon 440-746, Korea

Sei-Hoon Moon†
Department of Physics and Center for Theoretical Physics, Seoul National University, Seoul 151-742, Korea
(Received 2 March 1998; published 9 October 1998)

We study the axially symmetric static solitons of the O(3) nonlinear σ model coupled to (2+1)-dimensional anti–de Sitter gravity. The obtained solutions are not self-dual under a static metric. The usual regular topological lump solution cannot form a black hole even though the scale of symmetry breaking is increased. There exist nontopological solitons of half integral winding in a given model, and the corresponding spacetimes involve charged Bañados-Teitelboim-Zanelli black holes without non-Abelian scalar hair.
[S0556-2821(98)02420-5]

PACS number(s): 11.27.+d, 04.40.−b, 04.70.Bw

I. INTRODUCTION

Three-dimensional (3D) Einstein gravity is characterized by the absence of a propagating gravitational degree [1]. Though it is different from the nature of (3+1)-dimensional gravity, 3D gravity without the graviton has attracted attention in cosmology in connection with cosmic strings [2] and in the gauge theory formulation [3]. In both contexts, (2+1)-dimensional [(2+1)D] anti–de Sitter gravity may be intriguing because it was the first example reformulated as a Chern-Simons gauge theory of the Poincaré group [3] and its vacuum solutions support black holes [4].

(2+1)D gravity with a nonzero cosmological constant was first studied in Ref. [5]. When a static point particle with mass and without spin is coupled to gravity, a general anti–de Sitter solution was obtained:

$$ds^2=\sqrt{\varepsilon}\frac{\left(\frac{R}{R_0}\right)^{\sqrt{\varepsilon}c}+\left(\frac{R_0}{R}\right)^{\sqrt{\varepsilon}c}}{\left(\frac{R}{R_0}\right)^{\sqrt{\varepsilon}c}-\left(\frac{R_0}{R}\right)^{\sqrt{\varepsilon}c}}dt^2 - \frac{4\varepsilon c^2(dR^2+R^2d\Theta^2)}{|\Lambda|R^2\left[\left(\frac{R}{R_0}\right)^{\sqrt{\varepsilon}c}-\left(\frac{R_0}{R}\right)^{\sqrt{\varepsilon}c}\right]^2}, \tag{1.1}$$

where $c=1-4Gm$ and ε is ± 1 for the negative cosmological constant Λ. When $\varepsilon=+1$, the metric (1.1) describes a hyperboloid with a deficit angle. Note that the effect of the point particle at the origin appears only in the deficit angle in Eq. (1.1), and thereby these solutions go to vacuum solutions in the massless limit ($m\to 0$). Later Bañados-Teitelboim-Zanelli (BTZ) black hole solutions were reported in Ref. [4], and the simplest one is the Schwarzschild-type black hole

$$ds^2=(|\Lambda|r^2-8GM)dt^2-\frac{dr^2}{|\Lambda|r^2-8GM}-r^2d\theta^2. \tag{1.2}$$

Here an integration constant M of the Einstein equation is arbitrary; however, solutions of positive M correspond to BTZ black holes. Since both solutions in Eqs. (1.1) and (1.2) are vacuum solutions in the limit of zero point particle mass, one may easily find a coordinate transformation to connect the $m=0$ solutions in Eq. (1.1) with the solutions in Eq. (1.2). As expected, the $\varepsilon=+1$ case in Eq. (1.1) corresponds to the negative M solution in Eq. (1.2), and the corresponding space is a regular hyperboloid. The $\varepsilon=-1$ case results in the exterior region of the Schwarzschild-type BTZ black hole [6].

This BTZ black hole has so far attracted much interest in various classical black hole solutions [7], in thermodynamic and statistical properties [8,9], and in string-related topics [10]. In 3+1 dimensions, gravitating solitons and sphalerons have received considerable impetus by the discovery of a class of non-Abelian black hole solutions [11–13]. It might be an intriguing direction to ask the same question, that whether or not gravitating solitons in (2+1)D anti–de Sitter spacetime can form solitonic BTZ black holes. In the case of global U(1) vortices, a regular configuration could make a black hole structure with two horizons similar to the charged BTZ black hole [6]. Since the energy of a static global U(1) vortex diverges logarithmically in flat spacetime, we here want to address the same question to a model containing finite energy soliton excitations. In this context the O(3) nonlinear σ model may be an appropriate choice since the field content of the model is simple, and exact static self-dual multisoliton solutions of finite energy have been obtained in both flat [14] and curved spacetime with zero cosmological constant [15–17].

In this paper, we consider both the negative cosmological constant and matter distribution provided by regular static solitons of the O(3) nonlinear σ model. The metric of our consideration is static and axially symmetric. The inclusion of a negative cosmological constant leads us to expect to

*Electronic address: yoonbai@cosmos.skku.ac.kr
†Electronic address: jeollo@zoo.snu.ac.kr

induce a drastic change to solitonic physics in 2+1 dimensions. The role it plays is effectively equivalent to the introduction of angular momentum under a stationary metric, and then the corresponding spacetime provides a rotating frame to the test particle. Therefore, static σ solitons in anti–de Sitter spacetime cannot remain self-dual under the static metric. Even if we obtain self-dual σ solitons under the stationary metric, we encounter an unphysical situation, e.g., closed timelike curves [18]. An attractive gravitational force sounds natural in 3+1 dimensions for localized ordinary matter distributions, so that it makes the matter collapse into a black hole or coagulates a new localized object which does not exist in flat spacetime [11]. Since (2+1)D gravity itself does not contain a propagating gravitational field, negative vacuum energy can induce a similar effect in curved spacetime. In the O(3) nonlinear σ model, we present a new nontopological soliton solution of half integral winding in addition to the well-known topological lump solution of integral winding. We also show that any regular topological lump whose energy is localized near its core cannot form the spacetime of a BTZ black hole. However, nontopological solutions have a logarithmically divergent energy tail, so that their spacetimes can include charged BTZ black holes. In these aspects the obtained nontopological solitons resemble global U(1) vortices, but the non-Abelian scalar hair of σ solitons do not penetrate the horizon while the scalar hair of the global U(1) vortices can be observed outside the BTZ black hole.

This paper is organized as follows. In Sec. II, we introduce the model and obtain all possible static regular solitons with axial symmetry by solving second-order Euler-Lagrange equations. In Sec. III, the spacetime structure including BTZ black holes is analyzed for the obtained gravitating solitons. Geodesic motions are computed in Sec. IV. We conclude in Sec. V with a discussion.

II. MODEL AND SOLITON SOLUTIONS

The nonlinear σ model with O(3) symmetry is described by the Lagrange density

$$\mathcal{L}=-\frac{1}{16\pi G}(R+2\Lambda)+\frac{1}{2}g^{\mu\nu}\partial_\mu\phi^a\partial_\nu\phi^a -\frac{\lambda(x)}{2}v^2(\phi^a\phi^a-v^2), \tag{2.1}$$

where the Lagrange multiplier $\lambda(x)$ is rescaled to a dimensionless quantity, and the variation of it produces a constraint for the scalar field: $\phi^a\phi^a=v^2\ (a=1,2,3)$. Throughout this paper, the dimension counting of fields is adjusted to that in (3+1)-dimensional spacetime since we presume to apply the obtained results to straight, infinite strings. Then the model involves three mass scales, namely, the Planck scale $1/\sqrt{G}$, the scale of negative cosmological vacuum energy $\sqrt{|\Lambda|}$, and the symmetry-breaking scale v. Solitonic objects of our interest have axial symmetry; i.e., the corresponding string spacetime is invariant under the rotation to, and the translation along, a symmetry axis. The mass in this paper stands for mass per unit length along the symmetry axis. In this case the static metric of this spacetime can be parametrized as

$$ds^2=e^{2N(r)}B(r)dt^2-\frac{dr^2}{B(r)}-r^2d\theta^2-dz^2. \tag{2.2}$$

For this kind of metric all physical settings effectively reduce the hypersurface orthogonal to the symmetry axis, and the stringlike object can be viewed as a pointlike source in 2+1 dimensions. Suppose that a given matter distribution is specialized to the case of axially symmetric time-independent fields and the equations of motions are solved. The resulting metric has two integration constants that are identified as the mass and angular momentum [4]. Since we take a static metric (2.2) here, it is equivalent to set the angular momentum zero. When we fix the boundary condition at the origin for the fields and the metric, we will choose a value of the mass parameter $B(0)$ later. We take a stereographic projection for ϕ^a so that the ansatz for the solitons with axial symmetry is

$$\phi^a=v(\sin F(r)\cos n\theta,\sin F(r)\sin n\theta,\cos F(r)). \tag{2.3}$$

Euler-Lagrange equations derived from the action and the static metric are

$$\frac{d^2F}{dr^2}+\left(\frac{dN}{dr}+\frac{1}{B}\frac{dB}{dr}+\frac{1}{r}\right)\frac{dF}{dr}=\frac{n^2}{Br^2}\sin F\cos F, \tag{2.4}$$

$$\frac{1}{r}\frac{dN}{dr}=8\pi Gv^2\left(\frac{dF}{dr}\right)^2, \tag{2.5}$$

$$\frac{1}{r}\frac{dB}{dr}=2|\Lambda|-8\pi Gv^2\left\{B\left(\frac{dF}{dr}\right)^2+\frac{n^2}{r^2}\sin^2F\right\}. \tag{2.6}$$

A physical condition for the spacetime manifold is the reproduction of Minkowski spacetime in the limit of no matter ($T^\mu_\nu=0$) and zero cosmological constant ($\Lambda=0$), and then an appropriate set of boundary conditions is

$$B(0)=1 \quad \text{and} \quad N(\infty)=0. \tag{2.7}$$

When $n\neq0$, the scalar field ϕ^a in Eq. (2.3) being well defined forces the boundary condition at the origin such as

$$F(0)=0 \quad [\text{or} \quad \sin F(0)=0]. \tag{2.8}$$

Introducing a new variable $\tilde{r}=\ln r$ $(-\infty<\tilde{r}<\infty)$, we rewrite Eq. (2.4) as

$$\frac{d^2F}{d\tilde{r}^2}+\left(\frac{dN}{d\tilde{r}}+\frac{1}{B}\frac{dB}{d\tilde{r}}\right)\frac{dF}{d\tilde{r}}=\frac{n^2}{B}\sin F\cos F. \tag{2.9}$$

After eliminating derivative terms of the metric functions by use of Eqs. (2.5) and (2.6), we obtain

$$B\frac{d^2F}{d\tilde{r}^2}=n^2\sin F\cos F-(2|\Lambda|e^{2\tilde{r}}-8\pi Gv^2n^2\sin^2F)\frac{dF}{d\tilde{r}}. \tag{2.10}$$

From the vanishing of the right-hand side of Eq. (2.9) at spatial infinity, we read possible boundary values of the scalar amplitude:

$$F(\infty)=\begin{cases}\pi & \text{from the sine term,}\\ \pi/2 & \text{from the cosine term,}\\ \alpha(0<\alpha\leq\pi) & \text{from the } 1/B(\infty) \text{ term.}\end{cases} \tag{2.11}$$

The boundary condition in the last line of Eq. (2.11) comes from the divergence of $B(r)$ at spatial infinity. Precisely, $B(r)\approx|\Lambda|r^2$ for a sufficiently large r.

Before analyzing $n\neq0$ solutions of Eq. (2.4), we will show that there does not exist an $n=0$ regular nontrivial solution of this equation even in anti–de Sitter space. If we substitute Eqs. (2.5) and (2.6) into Eq. (2.4) when $n=0$, we obtain

$$\frac{d^2F}{dr^2}+\left(\frac{2\Lambda r}{B}+\frac{1}{r}\right)\frac{dF}{dr}=0. \tag{2.12}$$

Since $B(0)=1$, F given by a solution of this equation contains a logarithmic divergence at the origin, i.e., $F(r)\propto\int dr^2e^{-|\Lambda|r^2}/r^2$ for a sufficiently small r. Now that we have shown the nonexistence of the $n=0$ solution, let us look for the $n\neq0$ soliton solutions of Eqs. (2.4), (2.5), and (2.6) satisfying the boundary conditions in Eqs. (2.7), (2.8), and (2.11).

A. Topological soliton

Solutions satisfying the boundary condition that $F(0)=0$ and $F(\infty)=\pi$ are topological solitons when the base spatial manifold formed by them is topologically equivalent to two-dimensional Euclidean space. These static solitons are characterized by topological charge,

$$Q=\frac{1}{8\pi}\int d^2x\,\epsilon^{0ij}\epsilon^{abc}\phi^a\partial_i\phi^b\partial_j\phi^c \tag{2.13}$$

$$=\frac{n}{2}[\cos F(0)-\cos F(\infty)] \tag{2.14}$$

$$=n, \tag{2.15}$$

and this quantized charge n represents a winding number of the second homotopy group, that is, $\Pi_2(S^2)=Z$. From now on we will call topological solitons of this model ‘‘topological lumps.’’

The topological lumps are known to be unique static soliton species of the O(3) nonlinear σ model in flat spacetime, and they have been studied in curved spacetime as a candidate of global cosmic strings [15–17]. Since exact soliton solutions were obtained by solving the first-order self-dual equation, their existence has been automatic as far as the cosmological constant has not been taken into account. As we shall discuss it later, static solitons under the static metric

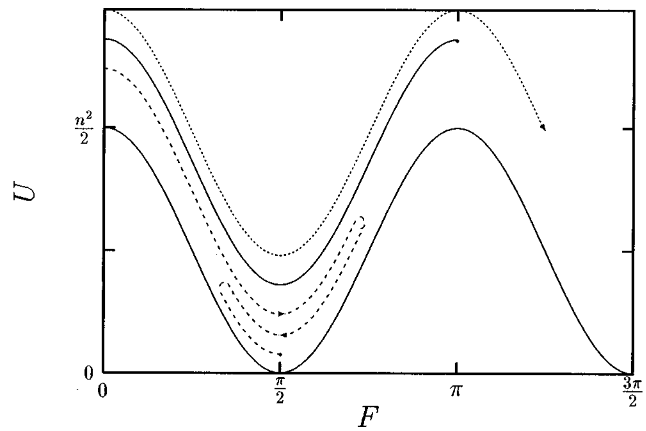

FIG. 1. Shape of the effective potential U and possible motions of a hypothetical particle: (a) overshoot solution (the dotted line), (b) critical solution with $F(\infty)=\pi$ (the solid line), and (c) undershoot solution with $F(\infty)=\pi/2$ (the dashed line).

are not self-dual in anti–de Sitter spacetime and then we have to consider the second-order Euler-Lagrange equation (2.4) directly.

Since we cannot exactly solve Eqs. (2.4), (2.5), and (2.6), let us attempt a series expansion of the fields near the origin:

$$F(r)\approx F_0r^n, \tag{2.16}$$

$$N(r)\approx N_0+4\pi Gv^2F_0^2nr^{2n}, \tag{2.17}$$

$$B(r)\approx1+\left[\frac{|\Lambda|}{v^2}-4\pi G(1+n^2)F_0^2\delta_{1,n}\right](vr)^2, \tag{2.18}$$

where F_0 and N_0 are constants determined by the proper behavior of the fields at the asymptotic region. For large r the leading term approximation gives

$$F(r)\approx\pi-\frac{F_\infty}{r^2}, \tag{2.19}$$

$$N(r)\approx-\frac{8\pi Gv^2F_\infty^2}{r^4}, \tag{2.20}$$

$$B(r)\approx|\Lambda|r^2+B_\infty+\frac{16\pi Gv^2|\Lambda|F_\infty^2}{r^2}, \tag{2.21}$$

where F_∞ and B_∞ are also determined by the proper functional behavior at the origin.

If we identify F as a coordinate and $\tilde{r}$ as time in Eq. (2.10), then we can interpret this equation as a Newtonian equation for the one-dimensional motion of a hypothetical particle with variable mass $B(r)$. The exerted forces are friction or a kind of velocity-dependent force proportional to $dF/d\tilde{r}$, and the conservative force from the potential $U=(n^2/2)\cos 2F$ (see Fig. 1).

If we naively read possible motions of a hypothetical particle from the potential $U(F)$, then the motions satisfying

$F(r=0)=0$ are classified into three sets by its initial velocity which can actually be replaced by the value of F_0 in Eq. (2.16). When F_0 is larger than a critical value, the particle reaches π at a finite time $\tilde{r}$ and it corresponds to an overshoot shown by the dotted line in Fig. 1. When F_0 is smaller than the critical value, the particle cannot reach π because of the power loss due to the velocity-dependent terms in Eq. (2.10) and this motion should have a turning point between $\pi/2$ and π. The existence of the overshoot solution given by the dotted line in Fig. 1 and the undershoot solution given by the dashed line in Fig. 1 guarantees, by continuity argument, the existence of the topological lump solution connecting $F(r=0)=0$ and $F(r=\infty)=\pi$ smoothly (see the solid line in Fig. 1).

For the metric functions, $N(r)$ is monotonically increasing since the right-hand side of Eq. (2.5) is always nonnegative; however, $N(r)$ is a slowly varying function in the asymptotic region as was shown in Eq. (2.20). It means that the exponential of $N(r)$ does not affect much the structure of spacetime. On the other hand, the functional behavior of $B(r)$ changes drastically according to both the magnitude of the cosmological constant and the matter distribution. Therefore, its spacetime structure, e.g., a black hole, is determined by reading the shape of $B(r)$. We will discuss possible spacetimes generated by various σ solitons in the next section.

In the above discussion, we neglected the effect of the variable mass $B(r)$ in Eq. (2.10). It may be valid when the absolute value of the cosmological constant is small. On the other hand, if $|\Lambda|/v^2$ is large enough, terms proportional to the cosmological constant dominate even for some finite $\tilde{r}$ region. In the Newtonian equation (2.10), such terms are interpreted as the variable mass term $B(\tilde{r})\sim|\Lambda|e^{2\tilde{r}}$ and the time-dependent coefficient of the friction $2|\Lambda|e^{2\tilde{r}}$ on the right-hand side of Eq. (2.10), respectively. In this case, the mass of the hypothetical particle can rapidly increase for small r and it can forbid the existence of overshoot solutions even for huge F_0 values. It is indeed the case which was confirmed by numerical computation. In synthesis, there exists a regular topological lump solution satisfying the boundary conditions $F(0)=0$ and $F(r=\infty)=\pi$ only when $|\Lambda|/v^2$ is less than a critical value. An example of the topological lump is shown in Fig. 2.

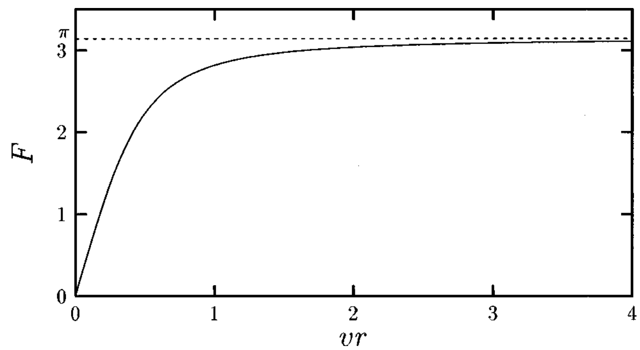

FIG. 2. A configuration of topological lump solution when $8\pi G v^2=0.2$, $|\Lambda|/v^2=4.0\times10^{-6}$, and $F_0=5.896$. The boundary value of the topological lump solution has π with 10^{-6} precision.

B. Nontopological soliton

When we discussed solutions of Eq. (2.11) in the previous subsection, we discussed the possibility of another set of regular solutions satisfying $F(\infty)=\alpha$ $(0<\alpha<\pi)$ as given in Eq. (2.11). Suppose that there exist such solutions and we attempt a power series expansion of them for large r:

$$F(r)\sim\alpha-\frac{F_{\alpha,\infty}}{r^q}. \tag{2.22}$$

From Eqs. (2.5) and (2.6), we have

$$N(r)\sim-4\pi G v^2 q\frac{F^2_{\alpha,\infty}}{r^{2q}}, \tag{2.23}$$

$$B(r)\sim|\Lambda|r^2+1-8G\mathcal{M}_\alpha-8\pi G v^2 n^2\sin^2\alpha\ln r/r_{\tilde{c}}, \tag{2.24}$$

where $F_{\alpha,\infty}$ and $\mathcal{M}_\alpha$ are constants which have to be chosen by the proper behavior of $F(r)$ and $B(r)$ near the origin, and $r_{\tilde{c}}$ stands for the core radius. Inserting the series solutions (2.22), (2.23), and (2.24) into Eq. (2.4) of the scalar field, we have a relation for the leading term:

$$-q(q-2)\frac{|\Lambda|F_{\alpha,\infty}}{r^q}=\frac{n^2}{r^2}\sin\alpha\cos\alpha. \tag{2.25}$$

When $\alpha\neq\pi/2$ and $0<\alpha<\pi$, the functional behavior of the radial coordinate forces $q=2$ but then the equality cannot hold because of the vanishing of the left-hand side of Eq. (2.25). This implies the impossibility of a regular $F(\infty)=\alpha$ solution except the $F(\infty)=\pi/2$ solution. When the boundary value of F is $\pi/2$, the charge defined in Eq. (2.13) is a multiple of half, i.e., $Q=n/2$. Therefore, every solution of $F(\infty)=\pi/2$ is classified as a static nontopological soliton of half integral winding.

In the previous subsection we mentioned the existence of undershoot solutions, and they should be nothing but the solutions of $F(\infty)=\pi/2$. Here let us emphasize again the impossibility of this half integral winding solution in flat spacetime. Since $N(r)=0$ and $B(r)=1$ in flat spacetime, Eq. (2.9) depicts a one-dimensional motion of a hypothetical particle with unit mass of which the position is F at time $\tilde{r}$. The exerted force comes only from the conservative potential $U(F)$ shown in Fig. 1; so a virial theorem allows two regular solutions, i.e., the stopped motion $[F(\tilde{r})=0]$ or the motion satisfying $F(\tilde{r}=-\infty)=0$ and $F(\tilde{r}=\infty)=\pi$. In curved spacetime with zero cosmological constant, the velocity-dependent force is not a friction but it pushes the hypothetical particle outward. Moreover, the variable mass $B(r)$ of the particle decreases as time $\tilde{r}$ elapses. These two factors make turning of the hypothetical particle more difficult before $F=\pi$ and forbid the undershoot solution. Therefore,

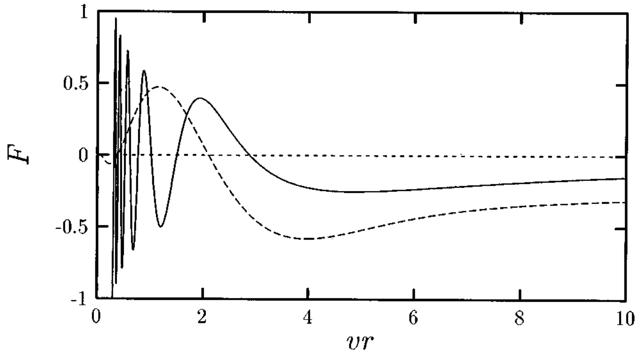

FIG. 3. Two types of asymptotic solutions for $\delta F(r) \equiv F(r) - \pi/2$ when $8\pi G v^2 = 0.4$ and $|\Lambda|/v^2 = 0.01$. The dashed line is a solution of Eq. (2.26) when $F_0 = 0.15$ and $F(r=0.01) = 0.0001$. The solid line is a solution of Eq. (2.27) when $F_0 = 10$ and $F(r=0.3) = -1$.

there does not exist any nontopological solitons of half integral winding in curved spacetime when the cosmological constant vanishes. In de Sitter spacetime, the positive cosmological constant term makes the situation worse; so we easily expect no half integral winding solution similar to the case of a zero cosmological constant. In anti–de Sitter spacetime, the negative cosmological constant term provides a friction as shown in Eq. (2.10) and lets the variable mass $B(r)$ get heavy for large r as given in Eq. (2.21). Among the solutions classified by the value of F_0 in Eq. (2.16), a set of F_0's less than the critical value for the topological lump solution provides a set of undershoot solutions with turning point between $\pi/2$ and π. Since the potential U has a minimum at $\pi/2$, it may oscillate around $\pi/2$ and finally converge to $\pi/2$ due to the friction.

For a better understanding of the asymptotic behavior of the scalar field $F(r)$, let us consider a linearized equation for $\delta F(r)$ defined by $F(r) = \pi/2 + \delta F(r)$. As an approximation of $B(r)$ we bring up two cases: One describes the region of slowly varying B $[B(r) \approx \bar{B}]$, and the other is the asymptotic region $[B(r) \approx |\Lambda| r^2]$. The former leads to

$$\bar{B} \frac{d^2 \delta F}{dr^2} + 3|\Lambda| r \frac{d\delta F}{dr} + \frac{n^2}{r^2} \delta F = 0, \qquad (2.26)$$

and the latter goes to

$$|\Lambda| r^2 \frac{d^2 \delta F}{dr^2} + 3|\Lambda| r \frac{d\delta F}{dr} + \frac{n^2}{r^2} \delta F = 0. \qquad (2.27)$$

A representative asymptotic solution of each equation is given in Fig. 3 and every solution includes both oscillation and damping as expected. Note that oscillations are rapid for small r but the period of each oscillation also increases rapidly as r increases. Since this small r region of rapid oscillation is covered by the soliton core, we may expect the possibility of a monotonic solution. It is indeed the case and we obtain a class of solutions specified by the number of $\pi/2$ points at finite r. From now on we will call this number a ''node.'' From the value of F_0 in Fig. 4 one may easily read

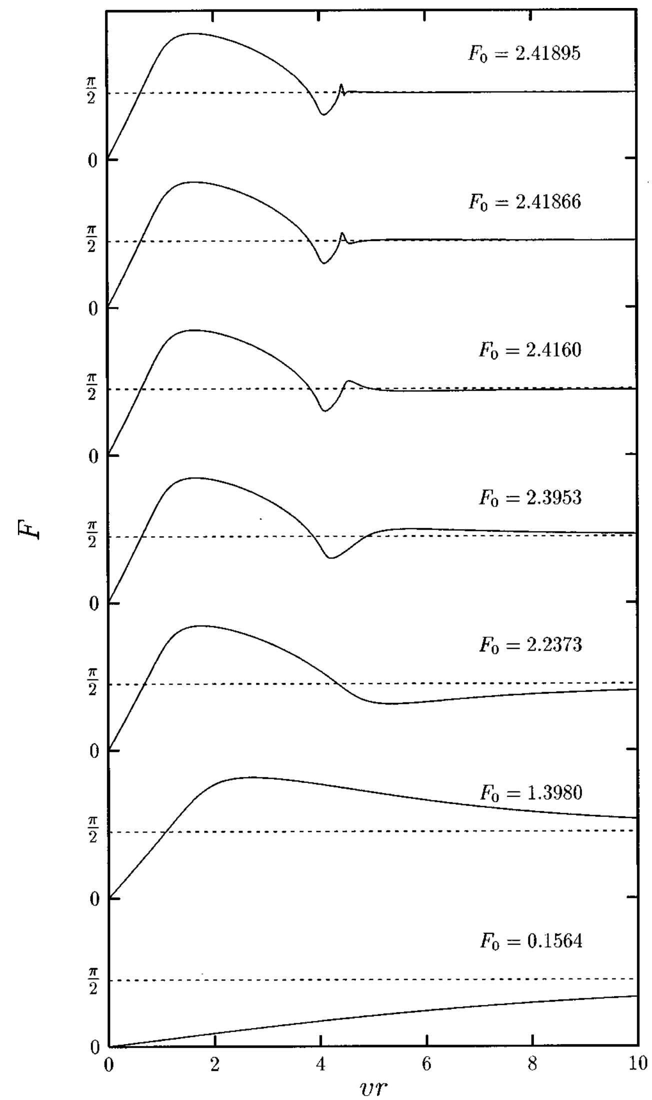

FIG. 4. Various nontopological solitons specified by the number of nodes when $8\pi G v^2 = 0.4$ and $|\Lambda|/v^2 = 0.01$.

proportionality between F_0 and the nodes. Obviously the maximum value of F also increases as F_0 becomes larger.

Now some comments on $B(r)$ for large r are in order. The expression (2.24) involves a logarithmic term when $\alpha = \pi/2$, and it means resemblance between the obtained nontopological solitons of half integral winding and the vortices in a scalar model with global U(1) symmetry [6]. The appearance of this logarithmic term also implies that the coordinate r may not be a good coordinate for the expansion of $B(r)$ in the asymptotic region as has been done in the global U(1) vortices [19,20].

It is well known that the O(3) nonlinear σ model in (2+1)D flat spacetime supports self-dual solitons described by the first-order equation

$$\partial_i \phi^a = \pm \frac{1}{v} \epsilon_i^j \varepsilon^{abc} \phi^b \partial_j \phi^c, \qquad (2.28)$$

and any static regular topological soliton with finite energy satisfying the Euler-Lagrange equation is proved to be self-dual and to satisfy Eq. (2.28). Here it would be natural to ask the question whether or not the obtained solutions in anti–de Sitter space are self-dual. In curved spacetime, the second-order equation from the self-dual equation (2.28) is

$$\nabla^2\phi^a-\frac{1}{v^2}(\phi^b\nabla^2\phi^b)\phi^a=\pm\frac{1}{v}\varepsilon^{abc}(\partial_j\epsilon^{ji}+\Gamma^j_{jk}\epsilon^{ki})\phi^b\partial_i\phi^c, \tag{2.29}$$

where ∇^2 denotes two-dimensional Laplacian. In the static metric (2.2), Eq. (2.29) becomes

$$B\frac{d^2F}{dr^2}+\left(B\frac{dN}{dr}+\frac{dB}{dr}+\frac{B}{r}\right)\frac{dF}{dr}-\frac{n^2}{r^2}\sin F\cos F =\pm\frac{1}{v}\frac{e^N}{r}\left(B\frac{dN}{dr}+\frac{1}{2}\frac{dB}{dr}\right)n\sin F. \tag{2.30}$$

Comparing Eq. (2.30) with the Euler-Lagrange equation (2.4), we obtain a necessary condition for the metric, that is, the vanishing of the right-hand side of Eq. (2.30):

$$\frac{dN}{dr}+\frac{1}{2B}\frac{dB}{dr}=0. \tag{2.31}$$

The solution of Eq. (2.31) with a rescaling of the time coordinate leads to

$$ds^2=dt^2-dz^2-\frac{dr^2}{B(r)}-r^2d\theta^2. \tag{2.32}$$

It is the very metric admitting self-dual stringlike solutions in curved spacetime with zero cosmological constant [15,16]. With the help of Eq. (2.31), Eqs. (2.5) and (2.6) are reduced to an equation

$$2|\Lambda|=-8\pi Gv^2\left(\sqrt{B}\frac{dF}{dr}-\frac{n}{r}\sin F\right)\left(\sqrt{B}\frac{dF}{dr}+\frac{n}{r}\sin F\right). \tag{2.33}$$

Since the (anti-)self-dual solitons satisfying Eq. (2.28) make the right-hand side of Eq. (2.33) vanish, we have $\Lambda=0$ as a necessary condition for any (anti-)self-dual soliton. Therefore, the static stringlike topological and nontopological configurations of the O(3) nonlinear σ model under the static metric (2.2) cannot saturate the Bogomolnyi-type bound in (anti–)de Sitter spacetime. In fact static self-dual solitons of this model with a cosmological constant were proved to be constructed only when the metric is stationary and the cosmological constant is negative [18].

In this section we analyzed the O(3) nonlinear σ model in anti–de Sitter spacetime and found a new static soliton configuration whose nature is nontopological, and its topological charge is a multiple of half integer in addition to the well-known topological lump solution. The obtained solitons are shown to be non-self-dual.

III. SPACETIME STRUCTURE

We have obtained in the previous section all possible static regular soliton solutions of Eq. (2.4), Eq. (2.5), and Eq. (2.6). In this section we address the question about possible spacetime manifolds formed by σ soliton configurations and a negative vacuum energy. Among the known (2+1)D anti–de Sitter spacetime solutions intriguing ones are the regular hyperboloid and BTZ black hole [5,4]. In Ref. [6], one of the authors showed that a static global U(1) vortex can form a space with two event horizons, which resembles a charged BTZ black hole. Specifically, what we are looking for is the existence of a black hole horizon, which is manifested by the region of nonpositive $B(r)$.

At first let us investigate the structure of spatial manifolds by the topological lump solutions and show that any regular topological lump configuration does not form a BTZ-type black hole even when the magnitude of the negative cosmological constant is small and the symmetry-breaking scale is of the order of the Planck mass. From the asymptotic form of $B(r)$ in Eq. (2.21), one can easily read a necessary condition to have negative $B(r)$. When B_∞ is not negative, the series expansion (2.21) of $B(r)$ is always positive for large r and it implies the impossibility of the existence of the horizon. On the other hand, Eq. (2.18) tells the opposite possibility that $B(r)$ of an $n=1$ soliton can be zero at some r, if $4\pi G(B_0+n^2)F_0^2$ is much larger than the magnitude of the cosmological constant $|\Lambda|$. In order to clarify this issue let us examine the integral equations for $N(r)$ and $B(r)$ obtained from Eq. (2.5) and Eq. (2.6):

$$N(r)=-8\pi G\int_r^\infty ds s\left(\frac{dF}{ds}\right)^2, \tag{3.1}$$

$$B(r)=e^{-N(r)}\left\{2|\Lambda|\int_0^r ds s e^{N(s)} -8\pi Gv^2n^2\int_0^r ds\frac{e^{N(s)}}{s}\sin^2F+e^{N(0)}\right\}. \tag{3.2}$$

The first term in the square brackets of Eq. (3.2) describes the contribution of the negative vacuum energy and second term the core mass. In order to obtain a negative $B(r)$ region for some r, a small magnitude of the negative cosmological constant is favorable. Since the third term $e^{-N(0)}$ is of order 1, another necessary condition from the second term in Eq. (3.2) is the lower bound of the symmetry-breaking scale v which must be the Planck mass, i.e., $8\pi Gv^2\sim 1$. To evaluate the value of B_∞ in Eq. (2.21), we take a crude approximation such as

$$N(r)=0 \tag{3.3}$$

and

$$F(r)=\begin{cases}0 & \text{for } 0<r<r_c-\Delta,\\ \pi/2 & \text{for } r_c-\Delta\leqslant r\leqslant r_c+\Delta,\\ \pi & \text{for } r>r_c+\Delta.\end{cases} \tag{3.4}$$

Inserting Eqs. (3.3) and (3.4) into the integral equation (3.2) and comparing the result with Eq. (2.21), we obtain

$$B_\infty \sim 1 - 16\pi G v^2 n^2 \left(\frac{\Delta}{r_c}\right). \tag{3.5}$$

Since both r_c and Δ have the scale of the soliton core size and the ratio Δ/r_c is of order 1, we can confirm that the Planck scale as a symmetry-breaking scale is necessary to exhibit the horizon of a BTZ black hole.

Now let us assume that there exists a horizon at r_H. At each horizon a set of appropriate boundary conditions is

$$B(r_H) = 0, \tag{3.6}$$

$$\left.\frac{dF}{dr}\right|_{r_H} = \frac{\dfrac{v^2 n^2}{r_H^2}\sin 2F(r_H)}{16\pi G r_H\left(\dfrac{|\Lambda|}{4\pi G} - \dfrac{v^2 n^2}{r_H^2}\sin^2 F(r_H)\right)}. \tag{3.7}$$

Since $B(0)=1$ and $B(r)\overset{r\to\infty}{\longrightarrow}|\Lambda| r^2$,the region of negative $B(r)$ should be bounded and thereby the number of horizons should be even. We attempt a series solution near the horizon r_H to leading order:

$$F(r) \approx F(r_H) + \frac{\dfrac{v^2 n^2}{r_H^2}\sin 2F(r_H)}{16\pi G r_H\left(\dfrac{|\Lambda|}{4\pi G} - \dfrac{v^2 n^2}{r_H^2}\sin^2 F(r_H)\right)}(r - r_H), \tag{3.8}$$

$$N(r) \approx N(r_H) + \frac{1}{32\pi G r_H}\frac{\left(\dfrac{v^2 n^2}{r_H^2}\sin 2F(r_H)\right)^2}{\left(\dfrac{|\Lambda|}{4\pi G} - \dfrac{v^2 n^2}{r_H^2}\sin^2 F(r_H)\right)^2} \times (r - r_H), \tag{3.9}$$

$$B(r) \approx 8\pi G r_H\left(\frac{|\Lambda|}{4\pi G} - \frac{v^2 n^2}{r_H^2}\sin^2 F(r_H)\right)(r - r_H). \tag{3.10}$$

Suppose that there exists a region of negative $B(r)$ bounded by r_H^{in} and r_H^{out} $(r_H^{in} < r < r_H^{out})$. Then other necessary conditions are $dB/dr|_{r_H^{in}} < 0$ and $dB/dr|_{r_H^{out}} > 0$, and they lead to $|\Lambda|/4\pi G - [v^2 n^2/(r_H^{in})^2]\sin^2 F(r_H^{in}) < 0$ and $|\Lambda|/4\pi G - [v^2 n^2/(r_H^{out})^2]\sin^2 F(r_H^{out}) > 0$ by Eq. (3.10). However, now that $F(r)$ seems to be monotonically increasing from $F(0) = 0$ to $F(\infty) = \pi$ according to the argument on the terminology of Newtonian mechanics and the results of the numerical analysis, the negativity of the numerator of the second term in Eq. (3.8) forces a condition to $F(r)$, that the value of $F(r_H^{in})$ should be larger than $\pi/2$ and that of $F(r_H^{out})$ should be smaller than $\pi/2$. Therefore the above conclusion, i.e., $F(r_H^{in}) > F(r_H^{out})$, contradicts the monotonically increasing property of $F(r)$. Therefore we arrive at a no-go conclusion that the axially symmetric regular static topological lump solution in the O(3) nonlinear σ model cannot support a BTZ-type black hole with two horizons in anti–de Sitter spacetime.

Since we have proved that any $B(r)$ corresponding to a regular topological lump configuration cannot be negative, the remaining question for the nonexistence of the black hole horizon is to show the positivity of the minimum of $B(r)$. Again, let us assume that there exists a point r_H such that $B(r_H) = 0$ and this is the minimum value of B. Then the position of the horizon r_H and the value of $F(r_H)$ are determined in a closed form from Eqs. (2.4) and (2.6):

$$r_H = \sqrt{\frac{4\pi G v^2 n^2}{|\Lambda|}} \quad \text{and} \quad F(r_H) = \frac{\pi}{2}. \tag{3.11}$$

If there exists a regular solution to have $B(r_H) = 0$, one can try a series expansion around the horizon r_H such as

$$F(r) \approx \frac{\pi}{2} + f_1(r - r_H) + f_2(r - r_H)^2 + f_3(r - r_H)^3 + \cdots, \tag{3.12}$$

$$B(r) \approx B_2(r - r_H)^2 + B_3(r - r_H)^3 + \cdots. \tag{3.13}$$

After replacing the $N(r)$-dependent term in Eq. (2.4) by use of Eq. (2.5), we substitute Eq. (3.12) and Eq. (3.12) into the modified equations (2.4) and (2.6). A comparison of both sides of the equations results in the flatness of regular $F(r)$, i.e., $0 = f_1 = f_2 = f_3 = \cdots$. Since the scalar amplitude of the topological lump connects $F(0) = 0$ and $F(\infty) = \pi$ in this coordinate system, this flatness suggests the impossibility of the existence of any regular topological lump through the position of the horizon r_H such that $F(r_H) = \pi/2$ and $dB/dr|_H = 0$. However, Eqs. (3.12) and (3.13) do not exclude configurations of which F and dF/dr are continuous at the horizon but not necessarily have continuous higher derivatives. The topological lumps obtained by numerical works are unlikely to be these examples. However, the case of nontopological solitons seems to be different since our numerical works show that F is constant outside the horizon, i.e., $F(r) = \pi/2$ for any r which is equal to or larger than r_H. The nontopological soliton, therefore, can be free from the above argument which was applied to the regular topological lumps, and forms an extremal black hole with $F(r_H) = \pi/2$ which will lead to the phenomenon of no scalar hair. Combining with the previous proof, we conclude that any regular topological lump of the O(3) nonlinear σ model does not form the spacetime of a BTZ black hole irrespective of the values of $|\Lambda|/v^2$ and $8\pi G v^2$. Therefore, the shapes of $B(r)$ from the regular topological lump solutions are classified into two categories: one is monotonically increasing $B(r)$ and the other is convex down $B(r)$ (see Fig. 5).

The behavior of $B(r)$ given in Fig. 5 describes the structure of the spatial hypersurface of the (2+1)-dimensional spacetime. Since the metric is static, the spatial manifold is characterized by the circumference $l(r) \equiv 2\pi r$ and the radial

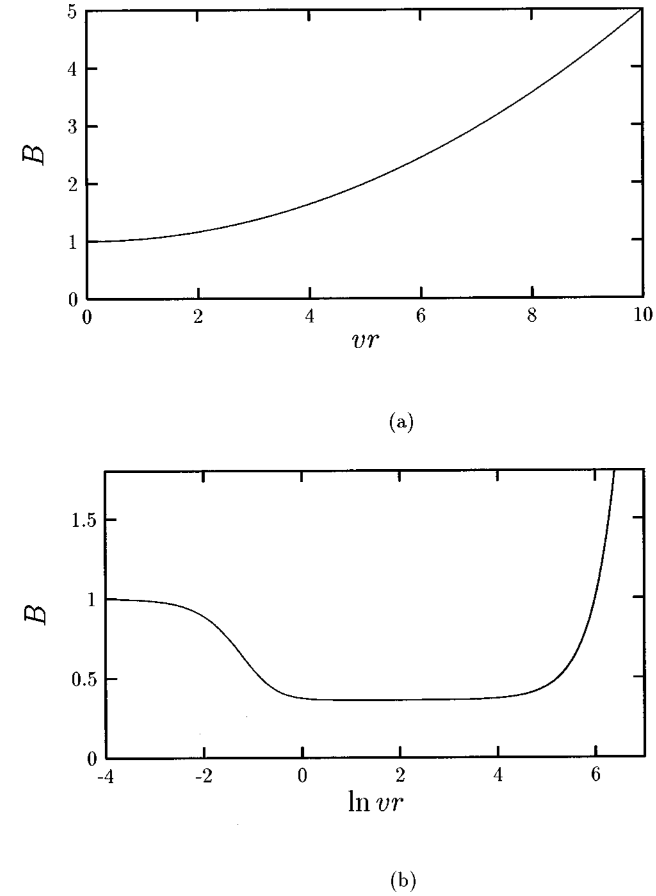

FIG. 5. Two characteristic shapes of $B(r)$ formed by the topological lumps: (a) a monotonically increasing $B(r)$ when $8\pi G v^2 = 8\times 10^{-8}$, $|\Lambda|/v^2 = 0.04$, and $F_0 = 1250$, and (b) a convex down $B(r)$ when $8\pi G v^2 = 0.2$, $|\Lambda|/v^2 = 4.0\times 10^{-6}$, and $F_0 = 5.896$.

distance $\mathcal{R}(r) = \int_0^r dr/\sqrt{B(r)}$. We embed it into a three-dimensional hyperbolic space by introducing a third axis Z such that $\mathcal{R}^2 = -Z^2 + r^2/B_m$, where $Z \geqslant 0$ and B_m is the minimum of $B(r)$. For sufficiently large r, $B(r) \sim |\Lambda| r^2 + B_\infty$ as given in Eq. (2.21). Introducing variables such as $\sqrt{|\Lambda|/B_\infty}\, r = \sinh\chi$ and $\sqrt{B_\infty}\,\theta = \Theta$, we obtain the asymptotic metric

$$ds^2 \approx \frac{1}{|\Lambda|}(d\chi^2 + \sinh^2\chi\, d\Theta^2). \tag{3.14}$$

The asymptotic region of the two-dimensional spatial manifold given by Eq. (3.14) is a hyperboloid with deficit angle $2\pi(1-\sqrt{B_\infty})$. By use of Eq. (3.5) we estimate the deficit angle to be $16\pi^2 G v^2 n^2$. This can easily be understood by the nonexistence of a long tail term in the energy-momentum tensor. Since nonvanishing independent components of it are

$$T^t{}_t = \frac{v^2}{2} B\left(\frac{dF}{dr}\right)^2 + \frac{n^2 v^2}{2r^2}\sin^2 F, \tag{3.15}$$

$$T^r{}_r = -\frac{v^2}{2} B\left(\frac{dF}{dr}\right)^2 + \frac{n^2 v^2}{2r^2}\sin^2 F, \tag{3.16}$$

they look to include a long tail term. However, substituting Eq. (2.19) into Eqs. (3.15) and (3.16), we read that the leading term is the $\mathcal{O}(1/r^4)$ term which does not affect the asymptotic region of the two-dimensional spatial manifold.

As we can expect from Fig. 5, the spatial manifold on the core of the topological lump is involved in one of two categories. When the absolute value of the negative cosmological constant is large enough, i.e., $|\Lambda|/v^2 > 8\pi G F_0^2 \delta_{1n}$ and $B_m = 1$, the relation between Z and r near the origin is $dZ \approx \sqrt{\alpha r^2/(1+\alpha r^2)}\,dr$ where $\alpha \equiv |\Lambda| - 8\pi G v^2 F_0^2 \delta_{1n}$. Then the core region of this soliton is also hyperbolic, $(Z + 1/\sqrt{\alpha})^2 - r^2 = 1/\alpha$. On the other hand, when $B(r)$ is decreasing near the origin, i.e., $|\Lambda|/v^2 < 8\pi G F_0^2 \delta_{1n}$ and $0 < B_m < 1$, the relation between Z and $r'(\equiv r/\sqrt{B_m})$ is given in the following:

$$Z(r) \approx \begin{cases} \sqrt{1-B_m}\, r'\left(1 + \dfrac{\alpha r'^2}{6(1-B_m)}\right) & \text{for small } r', \\ \sqrt{\dfrac{B_\infty}{|\Lambda| B_m} + r'^2} - \sqrt{\dfrac{B_\infty}{|\Lambda| B_m}} & \text{for large } r', \end{cases} \tag{3.17}$$

and

$$dZ \approx \sqrt{B_{m2}}(r' - r'_m)\,dr' \quad \text{around } r' = r'_m (\equiv r_m/\sqrt{B_m}), \tag{3.18}$$

where B_{m2} is the coefficient of the second-order term in the series of $B(r)$ around r_m. Since α is negative, the first line in Eq. (3.17) tells us that the core region is convex up. In order to connect smoothly the core and asymptotic regions of the spatial manifold, there should exist an inflection point about the minimum point r_m of $B(r)$ as given in Eq. (3.18).

From now on let us look into the possible structure of a spacetime manifold formed by the nontopological soliton of half integral winding. Recalling the asymptotic form of $B(r)$ in Eq. (2.24), one may easily notice a difference between this equation and Eq. (2.21) for the topological lump: The asymptotic space of the half integral winding soliton includes a logarithmic term with negative coefficient. This metric function is the same as that of a global U(1) vortex [6]. In the model of a complex scalar field the very logarithmic term has played a crucial role to constitute a vortex BTZ black hole with two horizons. On the other hand, our nontopological σ solitons are distinguished from global U(1) vortices by the following points. For a given model with fixed model parameters, the global U(1) vortex solution is unique; however, there are many nontopological σ soliton solutions characterized by the maximum value of the scalar amplitude which is larger than $\pi/2$ but smaller than π. About the shape of scalar amplitude, the former is a monotonically increasing

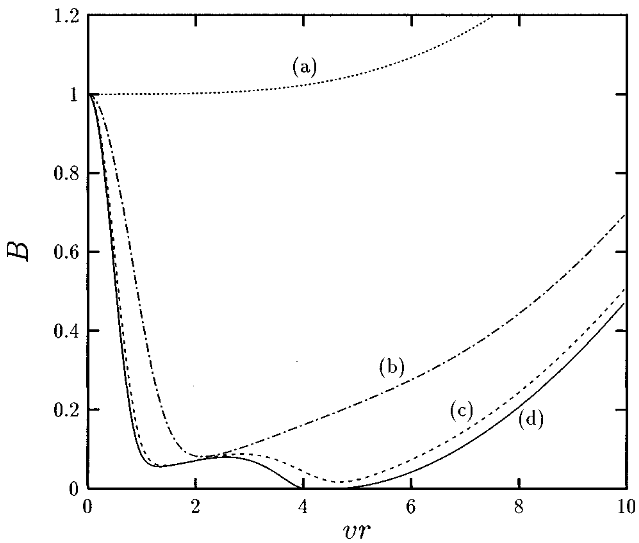

FIG. 6. Plots of $B(r)$ for various F_0's for $|\Lambda|/v^2=0.01$ and $8\pi Gv^2=0.4$: (a) zero node, (b) one node, (c) two nodes, and (d) extremal ($F_0=2.41902$ up to 10^{-6} precision).

function from zero to the vacuum expectation value but the latter can contain oscillatory behavior as shown in Fig. 4. Therefore, nontopological σ solitons with the same topological charge are classified into many subclasses by the number of nodes.

The existence of the logarithmic term in the asymptotic form (2.24) of the metric function $B(r)$ lets us ask an intriguing question about the generation of BTZ black holes for a small magnitude of the cosmological constant and relatively large symmetry-breaking scale as happened in gravitating global U(1) vortices with a negative cosmological constant. The results of the numerical analysis are summarized in Figs. 4 and 6. Figure 6 shows the metric B as a function of r for various numbers of nodes. As the number of nodes increases [or equivalently the value of F_0 in Eq. (2.16) increases], the value of the minimum of B decreases. It is also natural that the behavior of B is as like as Fig. 6 as the symmetry-breaking scale is increased with a fixed value of F_0. The nontopological σ soliton solutions are seen to tend towards black hole solutions as the symmetry-breaking scale v or the number of nodes is increased, as might be expected. A difference from the behavior of B for global U(1) vortices can be noticed: In case of the global U(1) vortices, one bump was dug and such a minimum of B finally touched a zero value [6]; however, several bumps are developed for nontopological σ solitons and the outmost one becomes the minimum of B and then this position tends to be a horizon as shown in Fig. 6. The graphs in Fig. 4 show that wiggles of the scalar field tend to subside to the boundary value $\pi/2$ outside the location of the minimum of B.

Within our numerical precision, a careful analysis of solutions near the transition to a black hole indicates that the nontopological σ soliton loses its scalar amplitude hair as it develops a horizon. In fact, it is predictable from Eq. (3.8): When $F(r_H)=\pi/2$, the actual value of $dF/dr|_{r_H}$ vanishes for any extremal black hole. Here let us write down the action (2.1) in terms of stereographically projected variables, i.e., $\phi^a=v(\sin F\cos(\Theta+\eta),\sin F\cos(\Theta+\eta),\cos F)$, where the multivalued Θ represents the topological sector and the single-valued function η the Goldstone degree for a given topological sector. Then, in (2+1)D flat spacetime, we obtain

$$\mathcal{L}=\frac{v^2}{2}[\partial_\mu F\partial^\mu F+\sin^2 F\partial_\mu(\Theta+\eta)\partial^\mu(\Theta+\eta)]. \tag{3.19}$$

By use of a duality transformation in 2+1 dimensions [21], one can easily show in the context of the path integral formulation that the above theory (3.19) is equivalent to that of a U(1) vector field A_μ:

$$\mathcal{L}=\frac{v^2}{2}\partial_\mu F\partial^\mu F-\frac{1}{4}\frac{F_{\mu\nu}F^{\mu\nu}}{\sin^2 F}+\frac{v}{2}\epsilon^{\mu\nu\rho}F_{\mu\nu}\partial_\rho\Theta, \tag{3.20}$$

where $F_{\mu\nu}=\partial_\mu A_\nu-\partial_\nu A_\mu$. If the scalar amplitude is frozen to be $F=\pi/2$, outside the black hole horizon, then the matter field action (3.20) is nothing but the sum of the Maxwell term and the minimal interaction between the gauge field and point particle. Now we understand the reason why a σ soliton black hole looks just like a charged BTZ black hole outside the horizon [4]. Therefore, nontopological σ solitons in the O(3) nonlinear σ model do not break the no-hair theorem. This phenomenon seems universal for our nontopological soliton solutions since it happens for a wide range of the symmetry-breaking scale v and the negative cosmological constant Λ. In this aspect, the regular nontopological σ solitons are also distinctive from the topological global U(1) vortices with scalar hair [6], but resemble the case of regular gravitating magnetic monopoles in 3+1 dimensions [12]. We can imitate the case of an exact singular monopole solution whose metric is the Reissner-Nordström black hole [22]. Specifically, $F(r)=\pi/2$, $\Theta=n\theta$, and $\eta=0$, everywhere and the corresponding black hole spacetime is a charged BTZ-type. More plausible singular configurations may be obtained by changing the boundary condition of the metric function at the origin, i.e., $B(0)\neq 1$, similar to the monopole black hole [12]. Since the singularity of the fields which is presumably at the origin can be hidden behind a horizon, we may not exclude the possibility that singular solutions can form small BTZ black holes lying within a nontopological σ soliton. Since no non-Abelian scalar hair can penetrate the horizon for regular solitons, we can evaluate the position of the horizon by using Eqs. (2.4) and (2.6), and it is nothing but the formula (3.11). The values of the horizon obtained by numerical analysis coincide with those from Eq. (3.11) within precision.

As usual, the matter distribution is reflected to the scalar curvature which is given by

$$R=-6\Lambda-16\pi GT^\mu_\mu. \tag{3.21}$$

For small r, Eq. (3.21) for both the topological lump and the nontopological soliton becomes

$$R \approx 6|\Lambda| - 8\pi G n^2 v^2 F_0^2 [2 + (|\Lambda| - 8\pi G v^2 F_0^2 \delta_{1,n}) r^2] r^{2n-2}. \tag{3.22}$$

When $n=1$, the curvature can be negative due to the accumulation of matter at the core of the soliton at the Planck scale. For large r, the behavior of the scalar curvature depends on the characteristic of the solitons:

$$R \approx \begin{cases} 6|\Lambda| - 32\pi G v^2 F_\infty^2 |\Lambda| \dfrac{1}{r^4} & \text{for the topological lump,} \\ 6|\Lambda| - 8\pi G v^2 n^2 \dfrac{1}{r^2} - 32\pi G v^2 |\Lambda| F_{\pi/2,\infty}^2 \dfrac{1}{r^4} & \text{for the nontopological soliton.} \end{cases} \tag{3.23}$$

As expected, the space is curved at large r for the nontopological soliton, while it is not for the topological lump. Although we have charged BTZ black holes from some half integral winding soliton configurations, we may expect that all the obtained spacetimes do not contain a physical curvature singularity due to the regularity of the matter fields and the metric functions everywhere. It is easily checked, by the Kretschmann scalar:

$$R_{\mu\nu\rho\sigma}R^{\mu\nu\rho\sigma} = 4G_{\mu\nu}G^{\mu\nu} = 4\,\mathrm{Tr}\left[\mathrm{diag}\left(-\frac{1}{2r}\frac{dB}{dr}, -\frac{1}{2r}\frac{dB}{dr} - \frac{B}{r}\frac{dN}{dr}, -\frac{1}{2}\frac{d^2B}{dr^2} - \frac{3}{2}\frac{dB}{dr}\frac{dN}{dr} - B\frac{d^2N}{dr^2} - B\left(\frac{dN}{dr}\right)^2\right)\right]. \tag{3.24}$$

When both $N(r)$ and $B(r)$ are regular everywhere, the only possible singularity can be at the origin in Eq. (3.24); however, it is also regular at the origin due to the behaviors of those metric functions at the origin as given in Eqs. (2.17) and (2.18). Then, the spacetime formed by the topological lump or the nontopological soliton is always regular everywhere irrespective of the existence of the black hole horizon.

As mentioned previously, we have many nontopological soliton excitations classified by the number of nodes for a given topological sector of the theory so that we have to discuss stability among these classical solutions carrying with the same topological charge. A good method is to compare their masses. Since the obtained spacetime is not asymptotically flat but is hyperbolic, the usual Arnowitt-Deser-Misner mass is not obtained in the limit $r \to \infty$. For the energy per unit length of infinitely long axially symmetric systems, known expressions are the C energy [23] and the conserved quasilocal mass [24]. Here we use the latter, the expression of which for the static observer is given by

$$M_q \equiv \frac{1}{4G}\sqrt{e^{2N(r)}B(r)}\,[\sqrt{|\Lambda|r^2+1} - \sqrt{B(r)}], \tag{3.25}$$

$$\overset{r\to\infty}{\longrightarrow} \begin{cases} 2\pi n^2 v^2 \left(\dfrac{\Delta}{r_{core}}\right) & \text{for the topological lump,} \\ \pi n^2 v^2 \left[\ln\left(\dfrac{r}{r_{core}}\right) + 2\sin^2\beta\left(\dfrac{\Delta}{r_{core}}\right)\right] & \text{for the nontopological soliton,} \end{cases} \tag{3.26}$$

where Eq. (2.21) was used on the right-hand side of the above expression. The mass for the topological lump has only the constant term. It is obvious because this lump is localized around its core without a long-range tail term. The nontopological soliton of half integral winding has a logarithmically divergent mass term in addition to the core mass. It shows some resemblance between the static global U(1) vortex and the nontopological soliton in the O(3) nonlinear σ model, whose leading long-range term is the same, i.e., $T_t^t \sim 1/r^2$ for large r.

For the $n=1$ class of solutions we compare the values of the quasilocal mass (3.25) of the no-node solution, one-node solution, two-node solution, the solution of an extremal black hole, and charged BTZ black hole at a sufficiently

TABLE I. The values of the quasilocal mass of various node solutions and the extremal charged BTZ black hole at a large distance $vr=50$ with $8\pi G=0.4$ and $|\Lambda|=0.01$.

node	0	1	2	extremal
$v=1$	0.01245	0.01918	0.02056	0.02080
$v=1.5$	0.02144	0.02625	0.02646	0.02647
$v=2$	0.02664	0.02840	0.02841	0.02841

large distance $vr=50$ as a function of v with fixed $8\pi G=0.4$ and $|\Lambda|=0.01$ (see Table I). The tendency that the quasilocal mass increases for higher node solutions looks universal, and further numerical studies for various G, $|\Lambda|$, and v also keep the same behavior. Therefore, the no-node solution is the lowest energy solitonic excitation among those with a given charge $n/2$. Since (2+1)D Einstein gravity does not have any attractive propagating gravitational degree, it seems natural. All half integral winding solitons are nontopological; so excited spectra may decay into the no-node soliton of the lowest energy. This procedure may presumably be correct for solitons in the space of a regular hyperboloid because the system has massless Goldstone degrees. Now, if we recall that the no-node solution with monotonically increasing $F(r)$ cannot form a black hole horizon, then an intriguing question is raised about the stability of an extremal BTZ-type black hole. In 3+1 dimensions, the attractive gravitational force usually makes a matter distribution with mass larger than the critical value unstable and leads to gravitational collapse where the destination is the formation of a black hole. It seems unlikely for our O(3) nonlinear σ model in (2+1)D anti–de Sitter spacetime. On the other hand, there may be an opposite procedure, that an extremal BTZ-type black hole is produced but it is energetically unfavorable and then the horizon disappears. However, we need further study on the stability of nontopological solitons to settle this issue. Now a comment about the critical symmetry-breaking scale is in order. In any natural environment the magnitude of the negative cosmological constant is much lower than the symmetry-breaking scale v, and the very symmetry-breaking scale v is much lower than the Planck scale. For example, if we consider the present universe with an extremely small bound of the negative cosmological constant ($|\Lambda|\sim 10^{-83}$ GeV^2), the critical value of the symmetry breaking not to form a BTZ-type black string is about 10^{-2} eV which is a very low energy. Of course, the above estimation is far from the realistic situation before we take into account the anisotropy in the cosmic ray background and other cosmological fluctuations.

IV. GEODESIC MOTIONS

The study of timelike and null geodesics is an adequate way to visualize the form of interaction on the soliton and the feature of its spacetime. Let us analyze possible geodesic motions and clarify whether a test particle experiences attraction or repulsion due to the soliton. The geometry depicted by Eq. (2.2) admits the rotational Killing vector $\partial/\partial\theta$ and the static Killing vector $\partial/\partial t$; so two corresponding constants of motion along geodesics are

$$\gamma=Be^{2N}\frac{dt}{ds} \quad \text{and} \quad L=r^2\frac{d\theta}{ds}, \tag{4.1}$$

where s is an affine parameter along the geodesic. Since the space is not asymptotically flat, the constant γ cannot be interpreted as the local energy of the test particle at infinity. The radial geodesic equation is

$$\frac{1}{2}\left(\frac{dr}{ds}\right)^2=-\frac{1}{2}\left[B(r)\left(m^2+\frac{L^2}{r^2}\right)-\frac{\gamma^2}{e^{2N(r)}}\right]=-V(r), \tag{4.2}$$

where the mass of the test particle can be rescaled as $m=1$ for timelike geodesics and $m=0$ for null geodesics. We analyze the trajectories of test particles for the topological lump background and the nontopological soliton background separately, and they are divided into four categories according to whether they have mass ($m=1$) or not ($m=0$), or whether their motions are purely radial ($L=0$) or rotating ($L\neq 0$). As shown in Fig. 5 and Fig. 6, the geometry of spatial manifolds of our σ model solitons is similar to those of global U(1) vortices [6]. Here we briefly mention different points.

A. Topological soliton

The main character of the spacetime structure of topological lumps is the absence of a black hole. Because of this character, the geodesic motions are simple. It is qualitatively similar to the regular hyperboloids by global U(1) vortices [6].

For the radial motion ($L=0$) of a massless test particle ($m=0$), the $B(r)$ dependence disappears in the effective potential $V(r)$. The allowed motion is an unbounded motion with speed $dr/ds=\gamma/\sqrt{2}$ at spatial infinity, only when $\gamma\neq 0$. Since $N(r)$ is monotonically increasing, this massless test particle in a radial motion always feels the attractive force.

For the rotational motions ($L\neq 0$) of a massless test particle ($m=0$), the effective potential includes the centrifugal force term $L^2B(r)/2r^2$ which forbids the test particle to access the soliton core. Therefore, any allowed rotational motion should have the minimum value of radius r_{min} that $r\geqslant r_{min}$. Since the value of the effective potential is $(|\Lambda|L^2-\gamma^2)/2$ at spatial infinity, any allowed motion should be bounded by the minimum radius r_{min} and the maximum radius r_{max} when $|\Lambda|L^2>\gamma^2$. However, we cannot see this easily due to the smallness of $|\Lambda|$. When $|\Lambda|L^2\leqslant\gamma^2$, the motions are also divided into two classes by the peak speed: One is the class with the peak speed at infinity, and the other is that with the peak speed at a finite radius.

The effective potential for the radial motion ($L=0$) of a massive test particle ($m=1$) is

$$V(r)=\frac{1}{2}\left(B(r)-\frac{\gamma^2}{e^{2N(r)}}\right). \tag{4.3}$$

For large r, it is approximated as

$$V(r) \approx \frac{|\Lambda|}{2} r^2 + \frac{1}{2}(B_\infty - \gamma^2) + \mathcal{O}(1/r^2), \tag{4.4}$$

and then all possible motions are bounded. Since the power series expansion of $V(r)$ for small r is

$$V(r) \approx \frac{1}{2}(1-\gamma^2 e^{-2N(0)}) + \left[\left(\frac{1}{2}|\Lambda| - 4\pi G v^2 F_0^2 (1-\gamma^2 e^{-2N(0)})\right) r^2\right] + \cdots, \tag{4.5}$$

we divide the shapes of the potential (4.3) into two classes. When the negative vacuum energy dominates the repulsive force of the scalar field even at the core of the soliton, i.e., $|\Lambda|/2 - 4\pi G v^2 F_0^2 (1-\gamma^2 e^{-2N(0)}) \geqslant 0$, $V(r)$ is monotonically increasing and thereby the force is attractive everywhere. Then the minimum of the effective potential is at the origin and its value is $|\Lambda|/16\pi G v^2 F_0^2$. The leading constant term in Eq. (4.3), which is the minimum of $V(r)$, tells us that radial motions are allowed only when $\gamma \geqslant e^{N(0)}$. On the other hand, when $|\Lambda|/2 - 4\pi G v^2 F_0^2 (1-\gamma^2 e^{-2N(0)}) \leqslant 0$, the test particle with γ smaller than the critical value γ_{cr} ($\gamma_{cr} = e^{N(0)} \sqrt{1-|\Lambda|/16\pi G v^2 F_0^2}$) feels the repulsive force at the core of the soliton. The allowed value of $V(0)$ lies between $|\Lambda|/16\pi G v^2 F_0^2$ and 1/2. One may expect that there exists a negative region of $V(r)$ between r_{min} and r_{max}; however, our numerical work shows the absence of such a region. Possible motions are (i) the stopped motion, (ii) the oscillation between the minimum radius and the maximum radius, and (iii) rolling to the origin, as γ decreases.

For the circular motions ($L \neq 0$) of a massive test particle ($m=1$), the effective potential takes general form [see Eq. (4.2)]. Since the centrifugal force term dominates at small r, $V(r)$ for small r resembles that of the case of a rotating motion of a massless test particle, and there exists a perihelion r_{min}. For large r, all motions are bounded by an aphelion r_{max} because of the negative cosmological constant term. The allowed motions are (i) the circular orbit at r_{circ} when $\gamma = \gamma_{circ}$ and (ii) the bounded orbit between the perihelion r_{min} and aphelion r_{max} when γ is larger than γ_{circ}. Noticing the vanishing of $V(r)$ at both r_{min} and r_{max}, one may suspect that the comoving time defined by

$$\tau = \int dr \frac{\gamma}{\sqrt{-2V(r)}} \tag{4.6}$$

diverges when the test particle approaches those points. However, since the denominator in Eq. (4.6) is proportional to $1/\sqrt{r-r_{min}}$ (or $1/\sqrt{r-r_{max}}$), it takes finite comoving time to reach a boundary and so does the coordinate time defined by $dt/d\tau = \gamma/Be^{-2N}$ since there is no black hole horizon, i.e., $B(r) > 0$ for all r.

B. Nontopological soliton

As we have discussed in the previous section, there exist black hole solutions for some nontopological solitons. For some regular solutions, e.g., (a) and (b) in Fig. 6, the geodesic motions are not so much different from those of topological solitons. There are different B's with several bumps as shown in graphs (c) and (d) in Fig. 6. One may suspect that these B's generate different geodesic motions, e.g., two isolated radial regions in the effective potential $V(r)$. However, our numerical works show that there is no such effective potential, so that the character of geodesic motions for regular nontopological solitons is the same as that for topological lumps. The only difference is the rapid variation of $V(r)$ near the origin, due to rapidly increasing $N(r)$. Note that Eq. (2.5) reflects the rapid increasing of $N(r)$ for many nodes of our nontopological soliton.

From Eqs. (4.1) and (4.2), the elapsed coordinate time t of a test particle which moves from r_0 to r is

$$t = \int_r^{r_0} \frac{dr}{B(r) e^{N(r)} \sqrt{1 - \frac{1}{\gamma^2}\left(m^2 + \frac{L^2}{r^2}\right) B(r) e^{2N(r)}}}. \tag{4.7}$$

It diverges when the test particle approaches a point where $B(r)$ vanishes at least linearly. As we expected, the spacetime with horizons depicts that of a black hole. For the black hole solutions, our geodesic motions outside the horizon are intrinsically the same with that of a charged BTZ black hole, since any scalar hair does not penetrate the horizon but the logarithmic Goldstone sector.

V. CONCLUSION AND DISCUSSION

In this paper we have studied static soliton solutions of the O(3) nonlinear σ model coupled to Einstein gravity with a negative cosmological constant. It has been shown that any regular static soliton configuration with an axially symmetric static metric is not self-dual in this anti–de Sitter spacetime. By examining second-order Euler-Lagrange equations, we obtained a new class of nontopological soliton solutions whose winding number is a multiple of half integer in addition to the well-known topological lumps with integral topological charge. The scalar amplitude of the topological lump solution is monotonically increasing according to numerical results, which interpolates the symmetric vacuum and the broken vacua, and its energy density, the time-time component of energy-momentum tenser, is localized around the soliton core. The lack of a long tail term in the energy density at the asymptotic region leads to the nonexistence of a BTZ-type black hole irrespective of the symmetry-breaking scale. The only spatial structure formed by the topological lump is a regular hyperboloid with a deficit angle.

On the other hand, the asymptotic behavior of the nontopological solitons shows an oscillation around its boundary value $\pi/2$, and these solutions are characterized by the number of nodes for a given parameter set of the model. The energy expressions of these nontopological solitons include a logarithmic term at the asymptotic region, and this property resembles that of global U(1) vortices. According to the scale of the negative cosmological constant, we obtained the following spacetimes: One of them is a regular hyperboloid with a deficit angle and the other is a charged BTZ black hole. The conserved quasilocal mass of the BTZ black hole is composed of two terms; i.e., one of them is the finite core mass and the other is a logarithmically divergent term.

Here we have several comments on some resemblance and difference between our half integral winding σ solitons and the global U(1) vortices. First, the former solutions are nontopological, but the latter solutions are topological. Therefore, the energetics of our nontopological solitons should be checked to confirm their stability, which may provide a clue to distinguish one from the other. Second, the global U(1) vortex is a unique regular soliton configuration with monotonically increasing scalar amplitude for a given set of model parameters. On the other hand, a number of nontopological solitons exist in a given model, which are characterized by the number of oscillations in the scalar amplitude. Third, both solitons carry a long range term ($\sim 1/r^2$) in the expressions of their energy density due to the nontrivial phase winding sector of Goldstone modes. The solutions have been seen to tend towards black holes as the symmetry-breaking scale increases and the magnitude of the negative cosmological constant becomes small. The black hole generated by a nontopological σ soliton is a charged BTZ black hole without non-Abelian scalar hair, while a small BTZ black hole lying within a global U(1) vortex is available where a nontrivial scalar field exists outside the horizon.

Since Einstein gravity in 2+1 dimensions does not have propagating degrees of freedom, the introduction of a negative vacuum energy plays a drastic role for making the soliton excitations rich in scalar theories. It made the global U(1) vortices free from the physical curvature singularity in the model of a spontaneously broken global U(1) symmetry. In our O(3) nonlinear σ model this attractive force supports the nontopological solitons, which have never been obtained without adding a gauge field and an explicit symmetry-breaking scalar potential [25] except for some unstable, spherically symmetric solitons in (3+1)D de Sitter spacetime [26]. The obtained spacetimes include charged BTZ black holes. In this context it may also be intriguing to ask the same question of local vortices in the Abelian Higgs model [27,28]. When we consider the stability of the obtained solutions or general straight infinite cosmic strings, various forms of the metric can also be taken into account, e.g., a metric with boost invariance along the string direction, $ds^2 = e^{2N(r)}B(r)(dt^2 - dz^2) - dr^2/B(r) - r^2 d\theta^2$, or the general form of static metric, $ds^2 = e^{2N(r)}B(r)[dt - C(r)dz]^2 - dr^2/B(r) - r^2 d\theta^2 - D(r)dz^2$, or even a stationary one, $ds^2 = e^{2N(r)}B(r)[dt - E(r)r d\theta]^2 - dr^2/B(r) - r^2 d\theta^2$.

Throughout this paper we have considered cases where the deficit angle is smaller than 2π. If we recall that supermassive local vortices produced various geometrical structures including an analogue of Kasner spacetime, a cylinder, or a two-sphere [28,29], we may expect some drastic change of (anti–de Sitter) spacetime formed by the topological lumps in the Planck scale. In relation to time-dependent soliton configurations, once the stationary Q-lump solution is generated and forms a black hole structure [30], it must be a spinning black hole in 2+1 dimensions.

Note added. After submitting this paper we became aware of Ref. [31], which is closely related to this paper.

ACKNOWLEDGMENTS

The authors would like to thank Chanju Kim and Kyoungtae Kimm for helpful discussions. This work was supported by the Ministry of Education (BSRI/97-2418), the KOSEF (Grant No. 95-0702-04-01-3 and through CTP, SNU), and Faculty Research Fund, Sungkyunkwan University.

[1] A. Staruszkiewicz, Acta Phys. Pol. **24**, 735 (1963); S. Deser, R. Jackiw, and G. 't Hooft, Ann. Phys. (N.Y.) **152**, 220 (1984); J. Gott and M. Alpert, Gen. Relativ. Gravit. **16**, 243 (1984); S. Giddings, J. Abbot, and K. Kuchar, *ibid.* **16**, 751 (1984).

[2] For a review, see A. Vilenkin and E. P. S. Shellard, *Cosmic Strings and Other Topological Defects* (Cambridge University Press, Cambridge, England, 1994); M. B. Hindmarsh and T. W. B. Kibble, Rep. Prog. Phys. **58**, 477 (1995).

[3] A. Achucarro and P. K. Townsend, Phys. Lett. B **180**, 89 (1986); E. Witten, Nucl. Phys. **B311**, 46 (1988).

[4] M. Bañados, C. Teitelboim, and J. Zanelli, Phys. Rev. Lett. **69**, 1849 (1992); M. Bañados, M. Henneaux, C. Teitelboim, and J. Zanelli, Phys. Rev. D **48**, 1506 (1993).

[5] S. Deser and R. Jackiw, Ann. Phys. (N.Y.) **153**, 405 (1984).

[6] N. Kim, Y. Kim, and K. Kimm, Phys. Rev. D **56**, 8029 (1997); Class. Quantum Grav. **15**, 1513 (1998).

[7] G. Clement, Phys. Rev. D **50**, 7119 (1994); Phys. Lett. B **367**, 70 (1996); K. C. K. Chan and R. B. Mann, Phys. Rev. D **50**, 6385 (1994); **52**, 2600(E) (1995); J. S. F. Chan, K. C. K. Chan, and R. B. Mann, *ibid.* **54**, 1535 (1996).

[8] S. Hyun, G. H. Lee, and J. H. Yee, Phys. Lett. B **322**, 182 (1994); K. Ghoroku and A. L. Larsen, *ibid.* **328**, 28 (1994); I. Ichinose and Y. Satoh, Nucl. Phys. **B447**, 340 (1995); S. Carlip and C. Teitelboim, Phys. Rev. D **51**, 622 (1995); M. Natsuume, N. Sakai, and M. Sato, Mod. Phys. Lett. A **11**, 1467 (1996).

[9] S. Carlip, Phys. Rev. D **51**, 632 (1995); M. Bañados, T. Brotz, and M. Ortiz, Report No. Imperial/TP/97-98/23, DFTUZ 98105, hep-th/9802076.

[10] N. Kaloper, Phys. Rev. D **48**, 2598 (1993); G. T. Horowitz and A. A. Tseytlin, Phys. Rev. Lett. **73**, 3351 (1994).

[11] R. Bartnik and J. McKinnon, Phys. Rev. Lett. **61**, 141 (1988).

[12] K. Lee, V. P. Nair, and E. Weinberg, Phys. Rev. Lett. **68**, 1100 (1992); Phys. Rev. D **45**, 2751 (1992); M. E. Ortiz, *ibid.* **45**, R2586 (1992); P. Breitenlohner, P. Forgács, and D. Maison, Nucl. Phys. **B383**, 357 (1992); T. Tachizawa, K. Maeda, and T. Torii, Phys. Rev. D **51**, 4054 (1995).
[13] For a review, see E. Weinberg, in *Proceedings of the 13th Symposium on Theoretical Physics*, edited by J. E. Kim (Min Eum Sa, Seoul, 1995); D. Maison, gr-qc/9605053; for the list of exotic black holes, see K. Maeda, J. Korean Phys. Soc. **28**, S468 (1995).
[14] A. A. Belavin and A. M. Polyakov, JETP Lett. **22**, 245 (1975).
[15] G. Clément, Nucl. Phys. **B114**, 719 (1976); A. Comtet and G. W. Gibbons, *ibid.* **B299**, 719 (1988).
[16] G. W. Gibbons, M. E. Ortiz, and F. Ruiz Ruiz, Phys. Rev. D **39**, 1546 (1989).
[17] G. W. Gibbons, M. E. Ortiz, and F. Ruiz Ruiz, Phys. Lett. B **240**, 50 (1990).
[18] Y. Kim and K. Kimm, Phys. Rev. D (to be published), gr-qc/9801063.
[19] R. Gregory, Phys. Lett. B **215**, 663 (1988); A. G. Cohen and D. B. Kaplan, *ibid.* **215**, 67 (1988).
[20] D. Harari and P. Sikivie, Phys. Rev. D **37**, 3438 (1988).
[21] R. L. Davis and E. R. S. Shellard, Phys. Lett. B **214**, 219 (1988); Y. Kim and K. Lee, Phys. Rev. D **49**, 2041 (1994).
[22] F. A. Bais and R. J. Russell, Phys. Rev. D **11**, 2692 (1975); Y. M. Cho and P. G. O. Freund, *ibid.* **12**, 1588 (1975).
[23] K. S. Thorne, Phys. Rev. **138**, B251 (1965).
[24] J. D. Brown and J. W. York, Phys. Rev. D **47**, 1407 (1993); J. D. Brown, J. Creighton, and R. B. Mann, *ibid.* **50**, 6394 (1994).
[25] K. Kimm, K. Lee, and T. Lee, Phys. Rev. D **53**, 4436 (1996); K. Arthur, D. H. Tchrakian, and Y. Yang, *ibid.* **54**, 5245 (1996).
[26] P. C. Aichelburg and C. Lechner, Phys. Rev. D **57**, 6176 (1998).
[27] D. Garfinkle, Phys. Rev. D **32**, 1323 (1985); A. Vilenkin, Phys. Rep. **121**, 263 (1985); W. Hiscock, Phys. Rev. D **31**, 3288 (1985).
[28] J. R. Gott III, Astrophys. J. **288**, 422 (1985); B. Linet, Class. Quantum Grav. **7**, L75 (1990); M. E. Ortiz, Phys. Rev. D **43**, 2521 (1991); C. Kim and Y. Kim, *ibid.* **50**, 1040 (1994); Y. Yang, Commun. Math. Phys. **170**, 540 (1995).
[29] P. Laguna and D. Garfinkle, Phys. Rev. D **40**, 1011 (1989).
[30] R. A. Leese, Nucl. Phys. **B366**, 283 (1991).
[31] G. Clément and A. Fabbri, Report No. GCR-98/04/01, gr-qc/9804050.